# Investigation of Electrodeposition of $Bi_2Te_3$ Nanowires into Nanoporous Alumina Templates with a Rotating Electrode

**Wen-Lin Wang,* Chi-Chao Wan, and Yung-Yun Wang**

*Department of Chemical Engineering, National Tsing-Hua University, 101, Section 2, Kuang Fu Road, Hsin-Chu, Taiwan, 300, Republic of China*

*Received: March 5, 2006; In Final Form: April 13, 2006*

A rotating electrode was employed to investigate the electrodeposition of $Bi_2Te_3$ nanowires. We found that mass transport of electrolytes into alumina templates of high aspect ratio plays a significant role in determining the properties of the obtained wires since diffusion is the rate-determining mechanism of mass transport within these nanochannels. In addition to slow growing rate, the effect of mass transport causes a slight composition variation from the bottom to the top of the wires. With a rotating electrode, the composition variation along the wires can be reduced by shortening the concentration depleted zone from the bulk electrolyte to the opening of pores. The wire growing rate can consequently be increased. Moreover, the wire compositions were confirmed to be adjustable by varying the rotation speed under the limitation of using a thin template.

## Introduction

Thermoelectricity is the phenomenon which results from forms of energy conversion (electricity to heat or vice versa). A good thermoelectric material should have high thermoelectric figures of merit, *Z*, which is defined by

$$Z = \alpha^2/\rho\lambda \quad (1)$$

where $\alpha$ is the Seebeck coefficient, $\rho$ the electrical resistivity, and $\lambda$ the thermal conductivity. The alloys of $Bi_2Te_3$ and their derived doped compounds are known to be the best thermoelectric materials below 100 °C since they possess features of high thermoelectric figure of merit (*Z*).[1−3] Other attractive properties of this material are its density (7530 kg/m$^3$), thermal conductivity (1.5 W/(m K)), specific heat (544 J/(kg K)), and thermal expansion coefficient ($13.0 \times 10^{-6}$/°C). Therefore, $Bi_2Te_3$ is an excellent candidate for preparing nanowires for thermoelectric applications.

At present, interest is focused on entirely different means of one-dimensional (1-D) nanostructures, such as nanowires and nanotubes since 1-D systems exhibit different transport properties of electrons and phonons.[4] In particular, dimensionality has become critical in thermoelectric materials because enhancement in thermoelectric efficiency has been reported for low-dimensional structures.[1−3] Therefore, much effort has been devoted to producing dense, ordered, and uniform $Bi_2Te_3$ nanowire arrays by electrodeposition.[5−9] By use of track etch alumina membranes as templates, electrochemical deposition of bismuth and tellurium within the channels could be realized by coating one side of the membrane with a conductive layer to serve as an electrode for the growth of material.[10,11]

The advantage of alumina membrane for nanowire array fabrication is its tunable pore dimensions over a wide range of diameters (10−300 nm) and lengths (over 100 $\mu$m).[12−14] In previous work, nanowire arrays of $Bi_2Te_3$ with different diameters ranging from 200[5] to 25 nm[6,7] have been successfully produced. Jin et al. have electrodeposited large area, high filling, and high aspect ratio nanowire arrays.[8] However, there are few reports pertaining to the influence of deposition conditions on the properties of wires. Electrodeposition of nanoporous structures with large area and high aspect ratios requires precise control of the alloy composition, the growing rate, and the structure of the deposit. Careful consideration should be given to uneven mass transport from the bulk electrolyte to the cathode surface at the bottom of pores for the electrodeposition process.

In this study, we focused on the influence of mass transport on electrodeposition into nanoporous alumina templates with a designed rotating electrode. Information thereby obtained could help us to analyze the mass transport during electrodeposition under well-defined hydrodynamic conditions. Under constant potential, we studied the compositions, the growing rate and the structures of nanowires produced under different stirring conditions. Furthermore, we also electrodeposited nanowire arrays under different polarization conditions without stirring for comparative purpose. Our ultimate aim is to produce uniform and dense $Bi_2Te_3$ nanowires of a well-controlled structure and composition by electrochemical techniques.

## Experimental Section

Alumina membranes 60 $\mu$m in thickness and 200 nm in pore diameter were purchased from Whatman International Ltd. The alumina membranes used in this study were all the same in dimensions and were commercially available since only the mass transport of electroactive species was involved and all the variances caused by alumina templates could be excluded. These membranes have a through-hole structure and are free from the barrier at the bottom. Before electrodeposition, a 2 $\mu$m thick platinum layer was sputtered onto one side of the membrane to serve as a working electrode. Due to perfect contact of deposit with the electrode surface, the resistance of barrier layer could be ignored.[15,16]

A piece of alumina membrane was first mounted on the rotating disk electrode (RDE) adaptor, as shown in Figure 1. The design of the adaptor basically follows the concept of

* To whom correspondence should be addressed. E-mail: d927604@oz.nthu.edu.tw. Tel: 886-3-5715131-33659. Fax number: 886-3-5715408.

10.1021/jp061362h CCC: $33.50 
Published on Web 06/06/2006

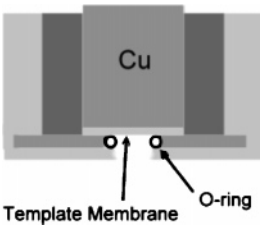


**Figure 1.** RDE adaptor for template membrane deposition.

**TABLE 1: Electrode Rotation Speed Dependence of the Wire Composition at the Bottom and the Top ($E = -0.14$ V vs SCE, 2 °C)**

| | | 400 rpm | 600 rpm | 800 rpm | 1000 rpm | 1400 rpm |
|---|---|---|---|---|---|---|
| bottom | % Bi | 42.35[a] | 41.85 | 42.83 | 42.98 | 44.32 |
| | | (36.36)[b] | (37.78) | (38.82) | (39.22) | (39.68) |
| | % Te | 57.65[a] | 58.15 | 57.17 | 57.02 | 55.68 |
| | | (63.64)[b] | (62.22) | (61.18) | (60.78) | (60.32) |
| top | % Bi | 44.87[a] | 44.25 | 43.86 | 44.59 | 45.33 |
| | | (38.52)[b] | (38.24) | (39.47) | (39.63) | (39.78) |
| | % Te | 55.13[a] | 55.75 | 56.14 | 55.41 | 54.67 |
| | | (61.48)[b] | (61.76) | (60.53) | (60.37) | (60.22) |

[a] $Bi^{3+} = 2.5$ mM and $HTeO_2^+ = 3.3$ mM. [b] $Bi^{3+} = 7.5$ mM and $HTeO_2^+ = 10$ mM.

Taephaisitphongse et al.[17] It allows a well-defined stirring state, which is necessary to control the electrolytes into the Nernst diffusion layer. Before deposition, the electrical contact resistance of the system was checked to make sure it was negligible. Moreover, linear sweep voltammetry was performed for determining an optimal potential at −0.14 V vs SCE for all rotating electrode experiments. $Bi_2Te_3$ nanowires were deposited electrochemically at 5 °C for $10^4$ s, which was under the control of a potentiostat (EG&G, PAR273).

All solutions were prepared from deionized water. Tellurium ion solutions were prepared from $TeO_2$ (SIGMA-Aldrich, 99+%) and bismuth ion solutions from $Bi_2O_3$ (Aldrich, 99.9%) in 1.0 M $HNO_3$. An electrolyte containing $Bi^{3+}$ and $HTeO_2^+$ was obtained from mixing the above solutions. In these electrolytes, there was an excess of $HNO_3$ as supporting electrolyte to minimize the migration effect.

Electron probe microanalysis (EPMA, JEOL JXA-8800M) was employed to measure the composition gradients of the deposited nanowires from the bottom to the top. To prepare samples for EMPA and X-ray diffraction (XRD) measurements, unfilled alumina templates, and the Pt-coated layers were mechanically polished away. Data from EPMA were collected from both sides of samples and repeated for 10 different sections on one piece of membrane. The quantitative results were reproducible within 2%. Among all the nanostructures tested, only the compositions at two ends of wires at a given deposition period were recorded. The level of filling could vary due to rate difference and could be observed by examining the field emission scanning electron microscopy (FE-SEM) images (Hitachi S-4700I) of the cross section of wire array. To prepare samples for study by SEM, the deposited membrane was first rinsed with water and ethanol thoroughly and then broken into pieces, exposing the lateral side of the membrane.

For transmission electron microscopy (TEM) observation, the alumina membrane was completely dissolved in a 2.0 M NaOH solution at room temperature for 24 h, then the resulting solution was sonicated for 5 min and then diluted with water and ethanol, sequentially. The high-resolution TEM (HRTEM) micrographs and the electron diffraction pattern were obtained by using TECNAI 20 Instruments at 200 kV. The X-ray diffraction pattern of the nanowires in the range of 20−80° was detected with a diffractometer (Rigaku, D/max-IIB) using Cu $K\alpha_1$ radiation.

## Results and Discussion

**(I) Deposition on a Rotating Electrode at Constant Potential.** Electrodeposition of nanoporous structures is different from that of macroscopic substrates. The alumina templates are assembly of tubular electrodes of 200 nm in diameter, partly covered by a nonconducting alumina layer with a depth of 60 $\mu$m. It thus can be viewed as an array of recessed nanoelectrodes.

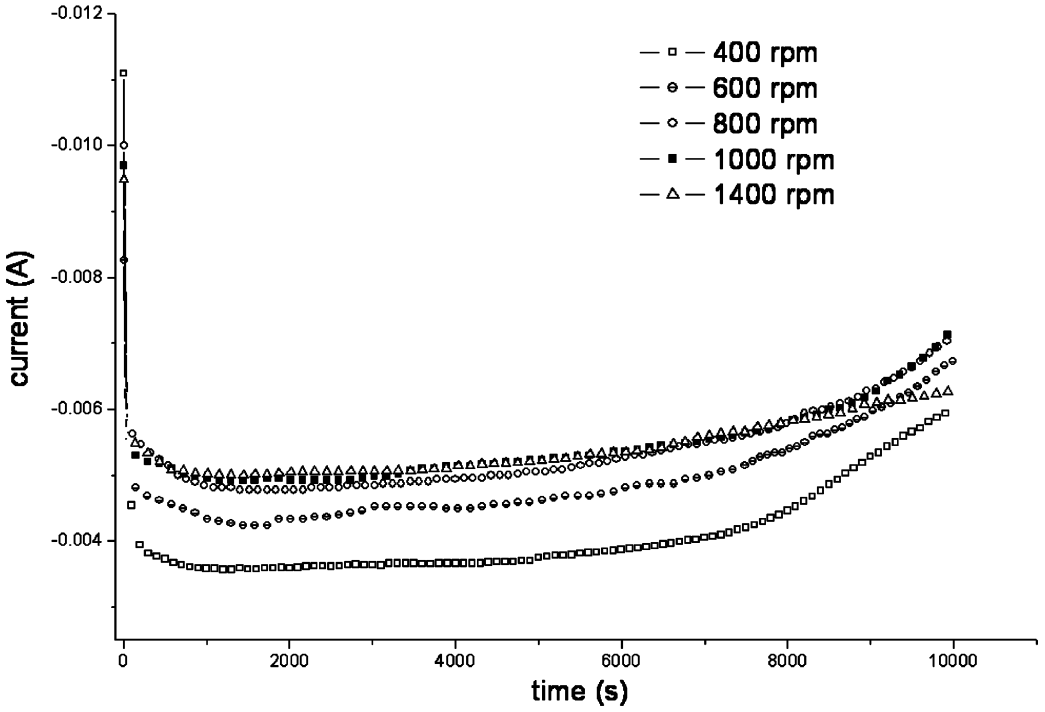


**Figure 2.** Current−time curve for the deposition of Bi/Te nanowires growing at −0.14 V vs SCE with a rotating disk electrode.

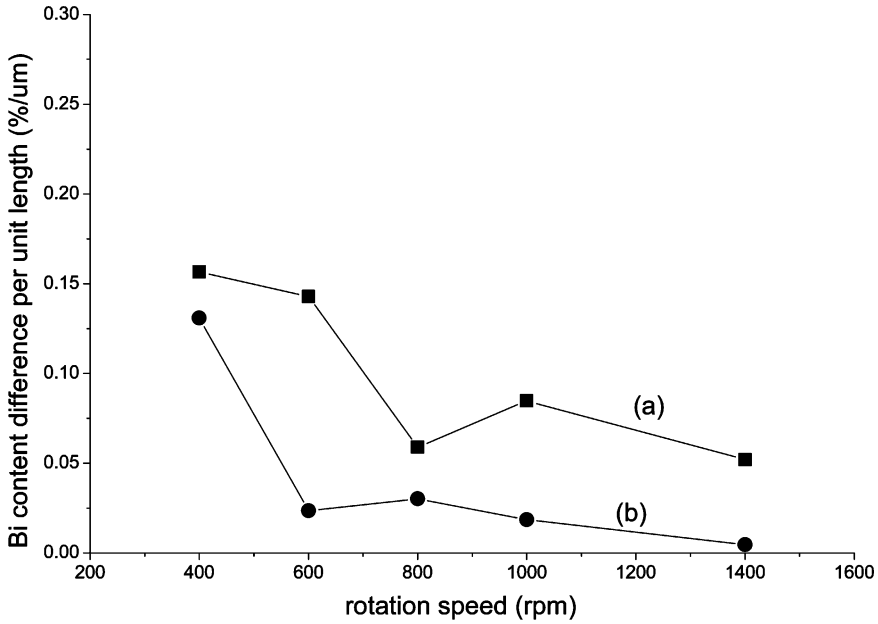


**Figure 3.** Composition variations over the length of Bi/Te nanowire arrays: (a) potentiostatically deposited at −0.14 V vs SCE with a rotating electrode ($Bi^{3+}$ = 2.5 mM and $HTeO_2^+$ = 3.3 mM); (b) potentiostatically deposited at −0.14 V vs SCE with a rotating electrode ($Bi^{3+}$ = 7.5 mM and $HTeO_2^+$ = 10 mM).

A model of the mechanisms of mass transport depending on lateral and vertical dimensions was proposed by Leyendecker et al.[18] They indicated that in a structure of high structural height (>500 um) and small pore diameter (<200 $\mu$m), the contribution of convection to mass transport can be neglected. In our case, the templates have the aspect ratio of 300 and the flow velocity in the normal direction to the pores is nearly zero. Therefore, diffusion is the rate-determining mechanism of mass transport within the template since it is hardly possible for convective flow to reach the bottom of the deep pores.

The current response of $Bi_2Te_3$ nanowires grown with a rotating electrode is shown in Figure 2. The rotation speed was varied between 400 and 1400 rpm. The high aspect ratio rendered a very low limiting current density compared to the plain substrate, meaning a restricted mass transport. There are two features in Figure 2. First, there is no linear relationship between the limiting current ($i_{lim}$) and the rotation speed ($\omega^{1/2}$) as theoretically predicted by the Levich equation.[19] The nearly constant limiting current obtained above 800 rpm indicates that the Nernst diffusion layer did not vary with rotation speed but was limited by the dimension of the alumina template. The phenomenon was also observed by Leyendecker et al. in their experiments with a rotating microstructure electrode (rme).[18] Second, while a diffusion layer was affected by hard templates, the practical distance for electrolyte flux diffusing to electrode surface would decrease as the wire grew in length. The current thus increased during the later stage of electrodeposition.

Typically, rotation of the electrode can directly affect the composition of the alloy by reducing the thickness of the cathodic diffusion layer.[20,21] However, from the above current−time curves, the diffusion layer for wire growth via template method was confirmed to be associated with the template height. To draw quantitative conclusions about the wire composition as a function of electrode rotation, a detailed analysis through the wire array is required. In this study, the Bi and Te content in the wires were determined by electron probe microanalysis. The detection limit of the instrument is 100 ppm (0.01 wt %),[22] and previous researchers in this field have commonly used EPMA for determining the composition differences of Bi−Te alloy.[23,24] The wire compositions were examined carefully in two aspects: the relation with the electrode rotation and with the wire length. All the results are listed in Table 1. The data in parentheses represent results obtained from an electrolyte of the same Bi/Te ratio but in a higher concentration. At the bottom of the wires, we can see that the composition of $Bi_2Te_3$ nanowires varied with the rotation speed of electrode in both diluted and concentrated solutions. Compared with the wire composition obtained under low rotation speed, the deposit contained more bismuth as the solution was more strongly stirred. Thus, without changing the deposition potential or the ratio of Bi/Te in solutions, the wire compositions can be controlled by our rotating electrode. This is a purely mechanical action which does not involve change of potential and electrolyte composition or the charge-transfer mechanism of the deposition process.

However, when we inspect the composition at the top of the wire also shown in Table 1, the variances among different rotation speeds were not so obvious. It indicates that at the later stage of electrodeposition, the contribution from electrode rotation to the diffusion layer thickness was indistinct, and the diffusion layer thickness was dominated mainly by the length of the channel within the template. That means wire composition control through rotation electrode has its own limitation and only applies to thin templates.

On the other hand, the composition gradient along the wire length can be represented by the differences of Bi content from the bottom to the top and then normalized by the corresponding wire length. The results are depicted in Figure 3. Curves a and b of Figure 3 describe the dependence of rotation speed on the difference of Bi content from two solutions. In curve a with a diluted solution, the difference was about 0.17%/$\mu$m at $\omega$ = 400 rpm and the value decreased with increasing rotation speed. In a concentrated solution as shown in curve b, Te-rich $Bi_2Te_3$ nanowires were obtained with the lower composition gradient. It is apparent that the composition gradient along the wires could be reduced by rapid stirring or by directly depositing in a concentrated solution. Both of them are closely related to mass transport of electrolytes.

In previous works on depositing $Bi_2Te_3$ thin film, the relation between ion diffusion and the film composition has been

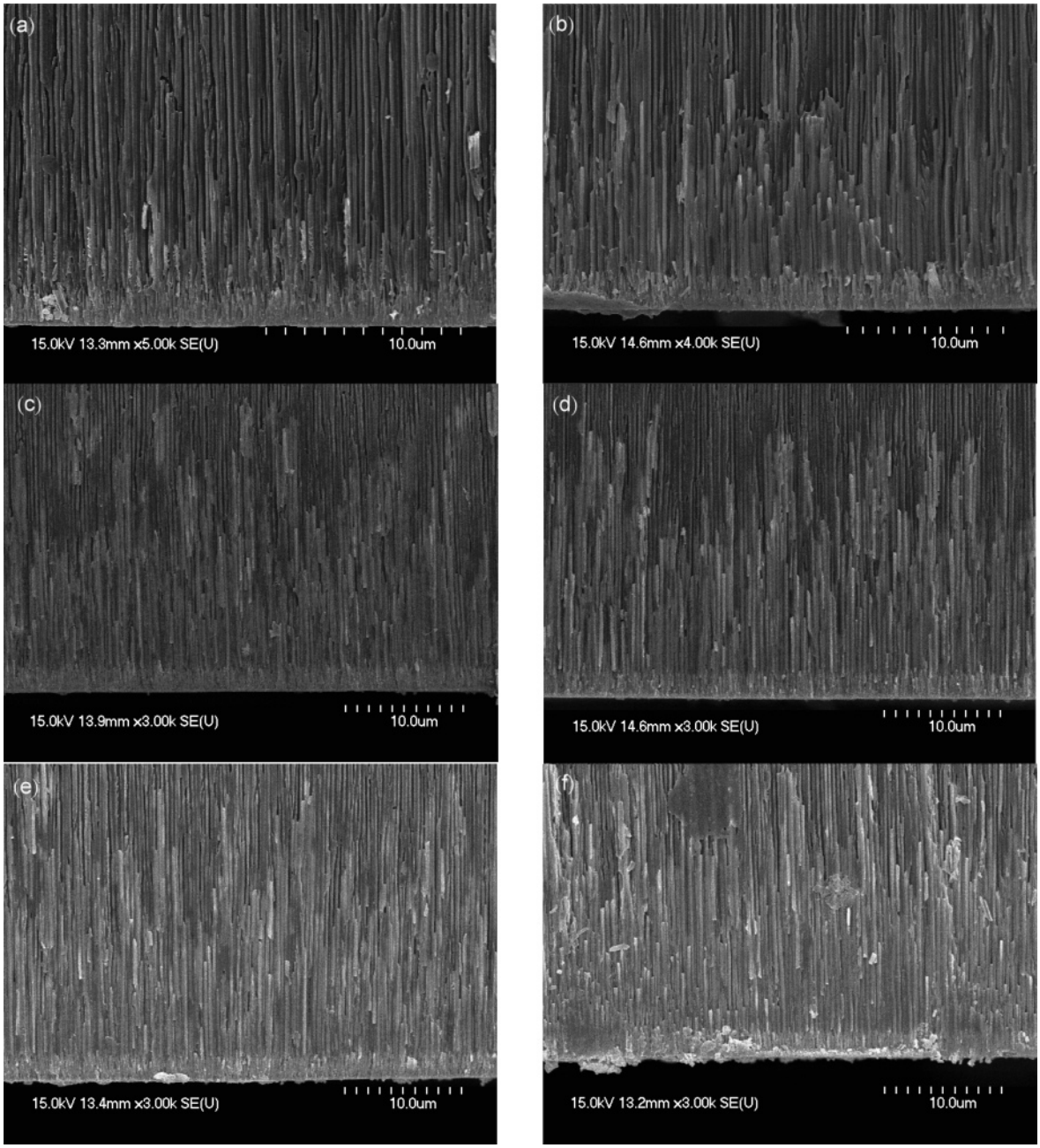


**Figure 4.** SEM images of cross section views of Bi−Te nanowire arrays showing different growing length depending on the electrode rotation speed at (a) 0, (b) 400, (c) 600, (d) 800, (e) 1000, and (f) 1400 rpm. Wires were deposited at −0.14 V vs SCE for $10^4$ s ($Bi^{3+}$ = 2.5 mM and $HTeO_2^+$ = 3.3 mM).

**TABLE 2: Cathodic Potential Dependence of the Wire Composition at the Bottom and the Top ($Bi^{3+}$ = 7.5 mM and $HTeO_2^+$ = 10 mM, $\omega$ = 0, 2 °C)**

| | | −0.14 V | −0.2 V | −0.3 V |
|---|---|---|---|---|
| bottom | % Bi | 35.99 | 36.25 | 39.18 |
| | % Te | 64.01 | 63.75 | 60.82 |
| top | % Bi | 37.93 | 39.71 | 49.03 |
| | % Te | 62.07 | 60.29 | 50.95 |

investigated.[21,24,25] Takahashi et al. have indicated that the limiting current of Bi−Te codeposition is limited by $Bi^{3+}$ diffusion.[25] Martín-González et al. suggested that the final composition of Bi−Te alloy depends strongly on $Bi^{3+}$ diffusion.[24] We also found in our previous research that Bi−Te codeposition is under diffusion control and the composition of the electrodeposited Bi−Te films is decided by the supply of electrolytes.[21] It means that the Bi−Te alloy composition is closely associated with mass transport of the electroactive species. In a structure of high aspect ratio, an uneven concentration profile arises from the bottom of pores to the bulk electrolyte in a mass-transfer-limited state. Thus, in response to the rate of mass transport, a composition gradient naturally appears along the wire during electrodeposition. Similar effects of mass transport at the bottom of gaps were found in electroforming of LIGA microstructures.[18,26,27] There was also a composition gradient present along the structural height.[26]

When a rotating electrode was employed for wire deposition, the reduction current from a structure of high aspect ratio (300 in our studies) could be viewed as the diffusion-limiting current. Although the thickness of diffusion layer does not vary with rotation speed, the importance of electrode rotation is demonstrated in the shortened concentration depleted zone from the bulk electrolyte to the opening of pores. It helps to maintain a

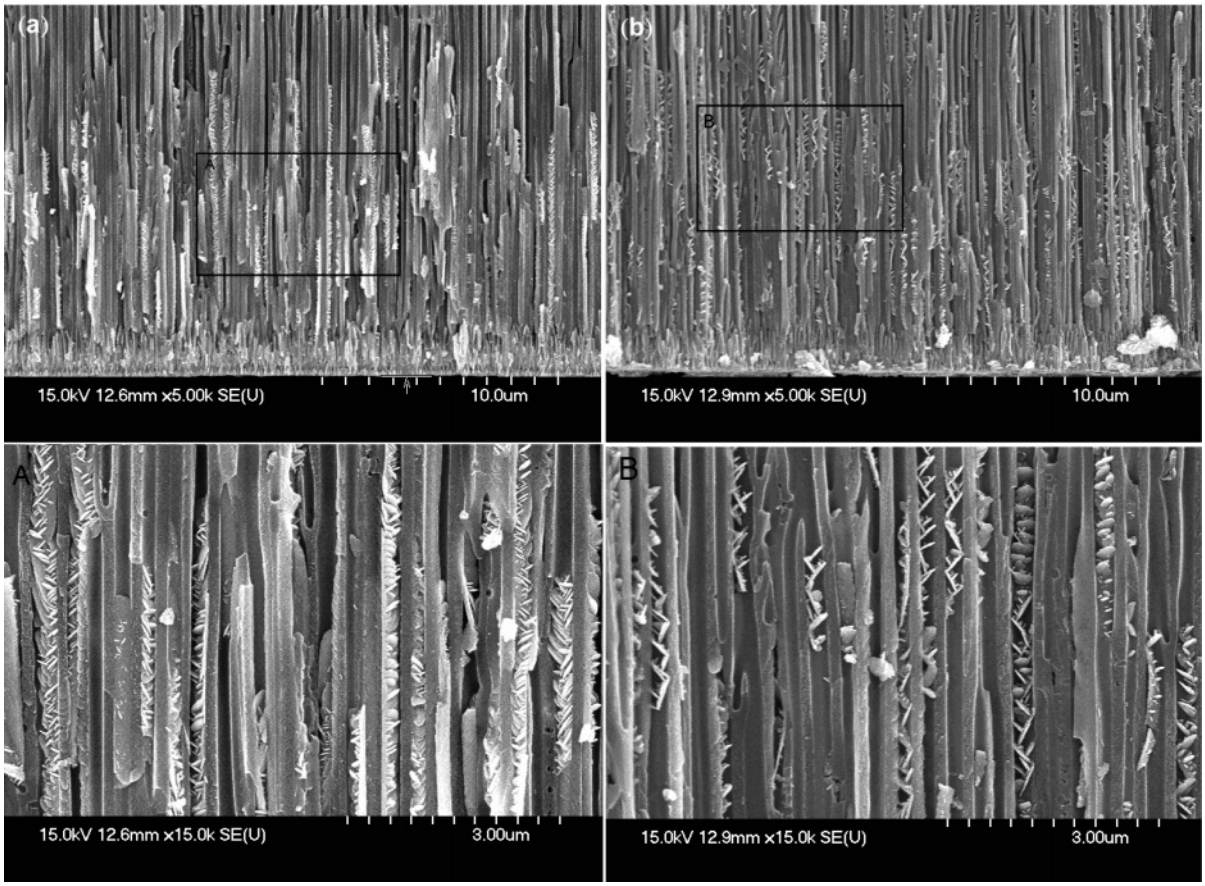


**Figure 5.** SEM images of cross section views of Bi−Te nanowire growing for $10^4$ s under the potential of (a) −0.2 V and (b) −0.3 V vs SCE. Images below are the magnified ones from the above. ($Bi^{3+}$ =7.5 mM and $HTeO_2^+$ = 10 mM.)

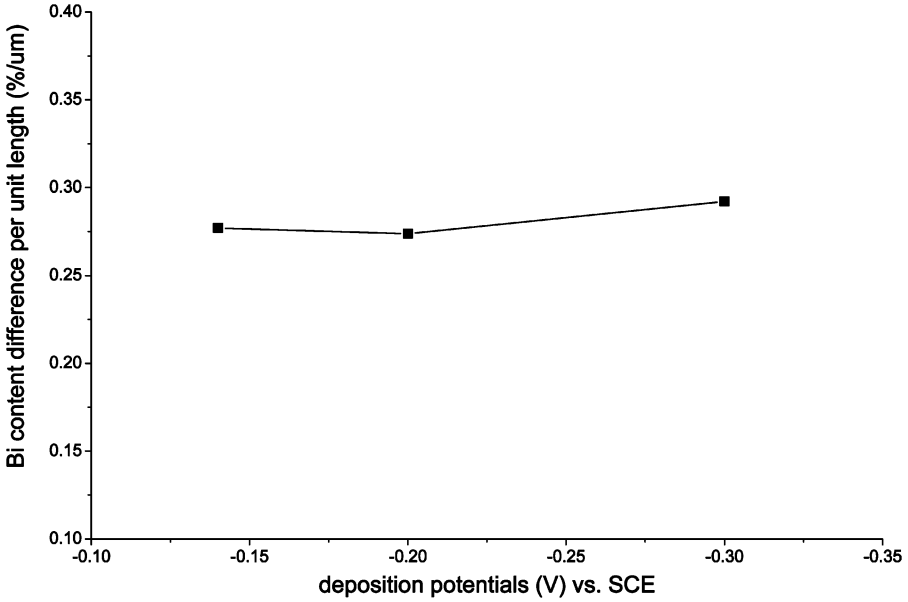


**Figure 6.** Composition variations over the length of $Bi_2Te_3$ nanowire arrays when deposited at different potentials in a static state ($Bi^{3+}$ =7.5 mM and $HTeO_2^+$ = 10 mM).

relatively uniform electrolyte concentration participating in the reaction. As a result, more homogeneous $Bi_2Te_3$ nanowire arrays can be fabricated by employing a rotating electrode in comparison to electrodeposition with a stationary electrode.

Figure 4 shows the SEM images of $Bi_2Te_3$ nanowire arrays within the alumina templates. The thin layer on the bottom represents the sputtered Pt, and the hill-like profile illustrates the uneven deposition distribution, so an average length was calculated from the SEM images. As mentioned above, low current density has to be used in practical application to electrodeposit nanoporous structure, rendering a slow growing rate. Indeed, if the electrode stayed stationary, the average wire length grown in a solution of 2.5 mM $Bi^{3+}$ and 3.3 mM $HTeO_2^+$ at −0.14 V for $10^4$ s was only ca. 5 $\mu$m. The growth rate can be increased to 16.1, 16.8, 17.5, 19, and 19.4 $\mu$m, while the electrode was rotated at 400, 600, 800, 1000, and 1400 rpm,

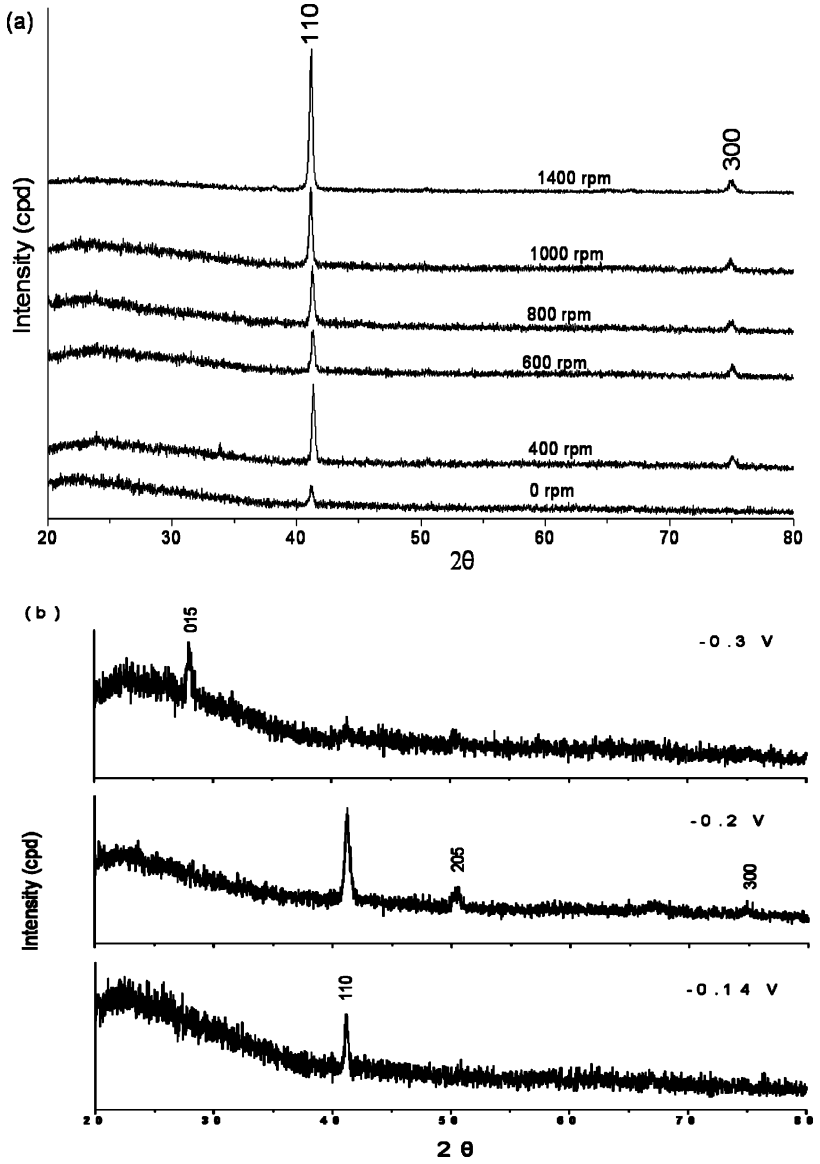


**Figure 7.** Comparison between XRD patterns of the Bi/Te nanowires obtained from (a) a rotating electrode with different rotation speeds, $E = -0.14$ V, and (b) different deposition potentials with a stationary electrode.

respectively. Using a rotating electrode to improve mass transport has allowed great increase in wire growing rate. Recently, Jin et al. have indicated that they can fabricate $Bi_2Te_3$ nanowires as long as ca. 20 $\mu$m within 2 h in a solution of high electrolyte concentrations, almost 15 times higher than the concentrations we used.[8] However, a high concentration electrolyte needs more acidic solution, which leads to concern about pore broadness on the alumina membrane.[15−16,28] With our rotating electrode, we can easily and efficiently achieve the same growing rate in a dilute and less acidic solution.

**(II) Deposition at Different Cathodic Potentials in a Stationary State.** The Bi−Te alloy compositions could also vary with changing cathodic current or potentials,[23−25,29−31] so it is possible to selectively prepare different types of $Bi_2Te_3$ nanowires by manipulating the polarized conditions. We thus studied the influence of cathodic potential on the properties of nanowires and then compared the results with those obtained with rotation. The electrodeposition was therefore performed in a stationary state.

First, increased polarization has led to faster growth of $Bi_2Te_3$ nanowires. The morphology of the wires grown at $E = -0.2$ and $-0.3$ V could be inspected from the FE-SEM images shown in Figure 5. The wire lengths are apparently longer than those obtained at $E = -0.14$ V shown in Figure 4a. However, the magnified images in Figure 5 indicate that a loose deposit structure appears within the template, which is common in rapid deposition under strongly polarized conditions.

The dependence of electrode polarization on wire compositions is shown in Table 2. We can see that the Bi content increased widely with the increased polarization. So, changing potentials is indeed a convenient method to adjust the wire composition. When examining the composition gradient along the wire, we found that the difference of Bi content increased from 0.276%/$\mu$m to 0.292%/$\mu$m when the potential was changed from $-0.14$ to $-0.3$ V vs SCE, as depicted in Figure 6. The enlargement in the difference of Bi content shows that mass transport exerts great influence on the wire composition in strongly polarized condition. Therefore, if the wire compositions are adjusted by changing deposition potentials, the effect of mass transport should be taken into consideration to preserve a well-defined result. Moreover, when comparing the curves in Figure 3 with the curve in Figure 6, we observe that the value of the difference of Bi content obtained from a stationary electrode is always larger than that from a rotating electrode. Thus, it again

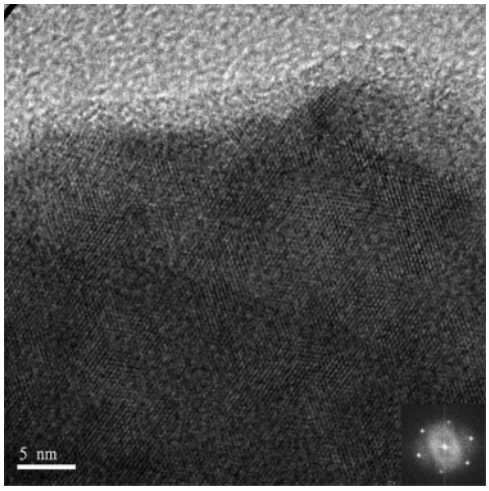


**Figure 8.** High-resolution TEM image of the $Bi_2Te_3$ nanowire produced via the rotation electrode. Rotation speed = 1400 rpm. The inset in the figure is the selected-area diffraction pattern.

indicates that the effect of mass transport can be minimized effectively by a rotating electrode.

**(III) Structure Analysis.** The XRD patterns of the as-prepared samples are shown in parts a and b of Figure 7 with rotation speed and cathodic potential as parameters, respectively. It is obvious that agitation of bath would not change the preferred growth direction and the dominant (110) peak of the hexagonal $Bi_2Te_3$ (PCPDF 15-0863) is most intensive (Figure 7a). However, increase in cathodic potential could change the orientation of the deposited crystals toward another closed packed plane, which was also observed by Miyazaki et al.[29] The (110) peak intensity appreciably decreases with the deposition potential leading to a deposit with an excess of Bi and an additional preferential growth direction appears. The nanowires grown at −0.3 V exhibit distinct (015) preferred orientation, as shown in Figure 7b.

A typical HRTEM image of a single nanowire prepared by the rotating electrode and corresponding diffraction pattern are shown in Figure 8. The lattice fringes apparent in this image indicate high crystallinity across this section of the nanowire. On the basis of the XRD results, the structures of the nanowires were strongly textured with the {110} planes perpendicular to the wire axis. With increasing rotation speed, steady electrolytes could diffuse into the cathode−solution interface, and the structure was thus more regular.

In summary, we have demonstrated the importance of mass transport in electrodeposition of $Bi_2Te_3$ alloy into nanoporous and high-aspect-ratio structure. A top technical challenge is to preserve a constant alloy composition and to achieve high deposition efficiency simultaneously in a mass-transfer-limited state. Also, the major concern of electrodeposition of $Bi_2Te_3$ nanowires for thermoelectric device application is the polycrystalline nature of the nanowires. A rotating electrode was found to be capable of shortening the concentration depletion zone from the bulk electrolyte to the opening of pores so that the depleted electrolyte can be replenished quickly. Consequently, the effects of mass transport are minimized. In addition to that, the structure of the nanowires has perfect crystallinity.

## Conclusions

The influence of mass transport on electrodeposition of $Bi_2Te_3$ nanowires into alumina templates has been demonstrated. We found that in a structure of high aspect ratio, diffusion is the rate-determining mechanism of mass transport. Due to slow mass transport, uneven concentration profiles within these nanochannels thus occur. It causes difference in wire composition from bottom to top. Agitation of bath by a rotating electrode can not only provide a nearly constant supply of electrolyte to the electrode surface but also increase the wire growing rate. As a consequence, ordered and uniform $Bi_2Te_3$ nanowires array can be obtained efficiently with our rotating electrode.

**Acknowledgment.** Support from the National Science Council of Taiwan is appreciated. NSC-942214E007008

## References and Notes

(1) Tritt, T. M. *Recent Trends in Thermoelectric Materials Research I−III*; Academic Press: San Diego, CA, 2001.

(2) Nolas, G. S.; Sharp, J.; Goldsmid, H. J. *Thermoelectrics-Basic Principles and New Materials Developments*; Springer: Germany, 2001.

(3) Rowe, D. M. *CRC Handbook of thermoelectrics*; CRC Press: Boca Raton, FL, 1995.

(4) Hu, J.; Odom, T. W.; Lieber, C. M. *Acc. Chem. Res.* **1999**, *32*, 435.

(5) Sapp, S. A.; Lakshmi, B. B.; Martin, C. R. *Adv. Mater.* **1999**, *11*, 402.

(6) Sander, M. S.; Prieto, A. L.; Gronsky, R.; Sands, T.; Stacy, A. M. *Adv. Mater.* **2002**, *14*, 665.

(7) Sander, M. S.; Gronsky, R.; Sands, T.; Stacy, A. M. *Chem. Mater.* **2003**, *15*, 335.

(8) Jin, C.; Xiang, X.; Jia, C.; Liu, W.; Cai, W.; Yao, L.; Li, X. *J. Phys. Chem. B* **2004**, *108*, 1844.

(9) Wang, W.; Huang, Q.; Jia, F.; Zhu, J. *J. Appl. Phys.* **2004**, *96*, 615.

(10) Martin, C. R. *Science* **1994**, *266*, 1961.

(11) Martin, C. R. *Chem. Mater.* **1996**, *8*, 1739.

(12) Masuda, H.; Hasegwa, F.; Ono, S. *J. Electrochem. Soc.* **1997**, *144*, L127.

(13) Masuda, H.; Yada, K.; Osaka, A. *Jpn. J. Appl. Phys.* **1998**, *37*, L1340.

(14) Müller, J. F.; Gösele, U. *Appl. Phys. Lett.* **1998**, *72*, 1173.

(15) Knaack, S. A.; Redden, M.; Onellion, M. *Am. J. Phys.* **2004**, *72* (7), 856.

(16) Crouse, D.; Lo, Y. H. *Appl. Phys. Lett.* **1998**, *76*, 49.

(17) Taephaisitphongse, P.; Cao, Y.; West, A. C. *J. Electrochem. Soc.* **2002**, *148*, C492.

(18) Leyendecker, K.; Bacher, W.; Stark, W.; Thommes, A. *Electrochim. Acta* **1994**, *39*, 1139.

(19) Bard, A. J.; Faulkner, L. R. *Electrochemical Methods*; John Wiley & Sons, Inc.: New York, 2001.

(20) Brenner, A. *Electrodeposition of Alloys*; Academic Press: New York and London, 1963; Vol. I.

(21) Wang, W. L.; Wang, Y. Y.; Wan, C. C. *J. Electrochem. Soc.* **2006**, *153* (6), C400.

(22) Goldstein, J. I.; Newbury, D. E.; Joy, D. C.; Lyman, C. E.; Echlin, P.; Lifshin, E.; Sawyer, L.; Michael, J. R. *Scanning Electron Microscopy and X-ray Microanalysis*; Plenum: New York, 2003; p 340.

(23) Michel, S.; Diliberto, S.; Boulanger, C.; Stein, N.; Lecuire, J. M. *J. Cryst. Growth* **2005**, *277*, 274.

(24) Martìn-Gonzàlez, M. S.; Prieto, A. L.; Gronsky, R.; Sands, T.; Stacy, A. M. *J. Electrochem. Soc.* **2002**, *149* (11), C546.

(25) Takahashi, M.; Oda, Y.; Ogino, T.; Furuta, S. *J. Electrochem. Soc.* **1993**, *140* (9), 2550.

(26) Bacher, W.; Menz, W.; Mohr, J. *IEEE Trans. Ind. Electron.* **1995**, *42*, 431.

(27) Romankiw, L. T. *Electrochim. Acta* **1997**, *42*, 2985.

(28) Piao, Y.; Lim, H.; Chang, J. Y.; Lee, W. Y.; Kim, H. *Electrochim. Acta* **2005**, *50*, 2997.

(29) Miyazaki, Y.; Kajitani, T. *J. Cryst. Growth* **2001**, *229*, 542.

(30) Magri, P.; Boulanger, C.; Lecuire, J. M. *J. Mater. Chem.* **1996**, *6* (5), 773.

(31) Tittes, K.; Bound, A.; Plieth, W.; Bentien, A.; Paschen, S.; Plotner, M.; Grafe, H.; Fischer, W.-J. *J. Solid State Electrochem.* **2003**, *7*, 714.